

Mechanical stability of nanoporous metals with small ligament sizes

Douglas A. Crowson, Diana Farkas* and Sean G. Corcoran

Department of Materials Science and Engineering, Virginia Polytechnic Institute and State University, Blacksburg, VA 24061, USA

Received 23 March 2009; revised 2 May 2009; accepted 4 May 2009

Available online 10 May 2009

Digital samples of nanoporous gold with small ligament sizes were studied by atomistic simulation using different interatomic potentials that represent varying surface stress values. We predict a surface relaxation driven mechanical instability for these materials. Plastic deformation is induced by the surface stress without external load, related to the combination of the surface stress value and the surface to volume ratio.

© 2009 Acta Materialia Inc. Published by Elsevier Ltd. All rights reserved.

Keywords: Porous material; Surface structure; Simulation

The corrosion process known as dealloying [1] has promise as a method to create nanoporous (np) metals for a variety of technological applications. Recently, a broad range of applications for these structures have been identified, including catalysts for fuel cells [2], and electrochemical actuators [3]. The ability to actuate np-Au was first reported in the literature by Kramer et al. [4]. The actuation is a result of varying the magnitude of the surface stress of the metal ligaments through application of an electrochemical voltage. This phenomenon was reported initially for thin polycrystalline ribbons of gold by Lin et al. [5]. Most recently, a number of papers have appeared in the literature focused on the various properties of np-Au, including actuation [6] and the effects of surface stress on material properties [7,8].

The main focus of this paper is to explore the morphological stability of nanoporous metals to capillary stresses by use of atomistic simulations. In order to better understand the stability of these structures, atomistic simulations of “model” np-Au were conducted as a function of surface stress and gold ligament diameter over the range $1.7\text{--}2.6\text{ J m}^{-2}$ and $1.3\text{--}3.6\text{ nm}$, respectively. The simulations shown here predict the initiation of plastic deformation at a critical value of the mean capillary pressure for a given value of the surface stress. Results for the 1.8 nm sample are presented in detail and demonstrate the initiation of plastic deformation at a surface stress value of 2.5 J m^{-2} .

Ideally we would directly use the experimentally rendered morphologies as input to atomistic modeling. We took advantage of the ease of generating spinodal-like morphologies with the desired periodic boundary conditions by use of phase-field calculations [8]. The phase-field structure was then scaled to match the mean wavelength and wavelength distribution desired. Figure 1 shows such a sample, including a comparison of the ligament size distribution with experimental distributions obtained by small-angle neutron scattering (SANS) and digitized scanning electron micrographs [9].

The sample presents regions of positive as well as negative surface curvature, similar to experimental observations.

The embedded atom method (EAM) potentials of Haftel and Rosen [10] were used for this study. This set of potentials was selected because they were designed to systematically vary the unrelaxed surface stress, thereby allowing us to probe surface stress effects on the relaxation and stability of nanoporous structures. The variation in surface stress of the potentials was achieved by progressively steepening the embedding function at electron density values typical of free surfaces (70–80% of bulk values). The potentials (Table 1) Au1–Au4 were generated from the initial potential, Au0, using this approach. The unrelaxed (1 0 0) surface stress (Table 1, column 2) varied up to 4 J m^{-2} which is comparable to first-principle values of $3.53\text{--}4.57\text{ J m}^{-2}$ [32] for the (1 0 0) surface [11,12]. The relaxed average surface stress values were obtained by performing energy minimizations of spherical particles of varying radius, r , using a standard conjugate gradient technique. A plot of radial strain, ϵ , vs. $1/r$ is linear with a slope

* Corresponding author. E-mail: Diana@vt.edu

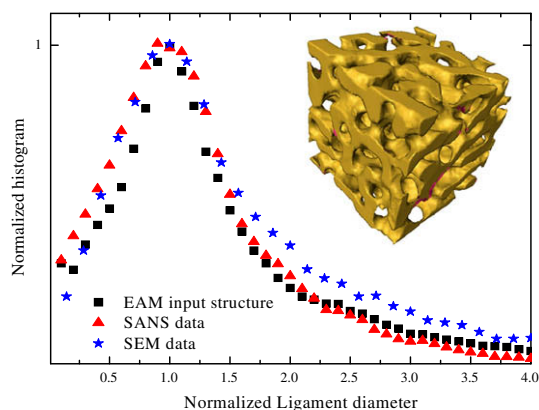


Figure 1. “Model” nanoporous gold. Surface plot rendering of an $18 \text{ nm} \times 18 \text{ nm} \times 18 \text{ nm}$ cube sample of np-Au used in the EAM simulations. The above sample contained approximately 200,000 atoms and had a average ligament size of 1.8 nm. The chord length distribution is compared to experimental samples characterized by small-angle neutron scattering and from thresholded scanning electron micrographs.

Table 1. Surface stress given by EAM potentials of HafTEL and Rosen [10]. Columns 2 and 3 give the values of the unrelaxed surface stress on the (1 0 0) and (1 1 1), while column 4 gives the results of the isotropic surface stress for relaxed spheres. All values are in J m^{-2} .

	Unrelaxed		Relaxed (sphere)
	(1 0 0)	(1 1 1)	
Au 0			1.703
Au 1	2.220	2.282	2.213
Au 2	2.891	3.786	2.525
Au 3	3.246	4.514	2.568
Au 4	4.063	6.282	2.379

proportional to the surface stress as given by $\varepsilon = -\frac{2\gamma}{3K} \frac{1}{r}$, where K is the bulk modulus. The results of these simulations are shown in column 4 of Table 1 and vary from 1.7 to 2.6 J m^{-2} . During the relaxation, surface reconstruction was observed only for the potential Au4.

Nanoporous Au structures with average ligament diameters of 1.3, 1.4, 1.5, 1.8, 2.1, 2.7 and 3.6 nm were generated as input for the atomistic calculations. The ligament sizes used here have some overlap with experimentally attainable sizes [9] and are small in order to keep the number of atoms in the simulation box relatively small. Small ligament sizes imply large capillary effects and therefore allow us to study cases where the effects of surface stress can be most significant.

The pore volume fraction for all of these structures was 0.5. Molecular dynamics (MD) equilibrations were then used to investigate the surface stress induced strains in these structures. The MD code LAMMPS [13] was used for these simulations on System X at the Terascale Computing Facility of Virginia Tech.

The samples were relaxed using an isothermal–isobaric ensemble (NPT) at 1 K and 0 mean pressure. The relaxations were performed in the following manner for each of the seven samples. The sample was first relaxed using potential Au0 (lowest f) until a stable value of the volumetric strain was achieved. The resulting structure was then relaxed with potential Au1 (increased

f), then Au2, etc. Figure 2 shows a slice through one sample in the initial configuration relaxed with Au0 and in the relaxed configuration obtained using the potential Au2, corresponding to an increased average surface stress of 2.5 J m^{-2} . In this figure the atoms are colored by the centrosymmetry parameter [14] where dark blue corresponds to the face-centered cubic bulk atoms, red corresponds to surface atoms and green corresponds to hexagonal close-packed stacking (appearing in stacking faults or twins). The arrows indicate dislocation activity induced by the increased surface stress, in the absence of any external loading.

For the particular case of the 1.8 nm ligament sample, the potentials Au0 and Au1 show complete elastic compression of the structure. The relaxation curves are shown in Figure 3, indicating an initial rapid jump in the volumetric strain; following this jump the volumetric strain remains stable. No dislocations or stacking faults were observed in the structure. With potential Au2 we see the first evidence of plastic deformation, as shown in Figure 2. The relaxation curve in Figure 3 in this case shows a period of relatively slowly increasing volumetric strain before a stable value is reached. This is indicative of a plastic deformation process, as can indeed be seen in the stacking faults that appear in the atomic structure of Figure 2.

Cycling of the potential back to Au1 and then returning to Au2 shows a recovery of only the elastic portion of the strain, and the potential can now be cycled between Au1 and Au2 with completely reversible strain amplitude. The relaxation with potential Au3 indicates a larger amount of plastic deformation. This is also evidenced by an increased stacking fault density observed in the images.

A plot of the critical relaxed surface stress to initiate plastic deformation vs. the volume to surface area ratio (V/S) is shown in Figure 4. These data follow the generalized capillary equation, $\langle f \rangle = \frac{3}{2} \langle P \rangle \frac{V}{S}$, where a linear relationship is observed between these two quantities, the slope of which is proportional to the mean pressure at which yielding is observed, 3.7 GPa in this case. This value is close to the theoretical shear strength and also is in agreement with the results of MD simulations of gold nanowires [15]. We note that a purely hydrostatic pres-

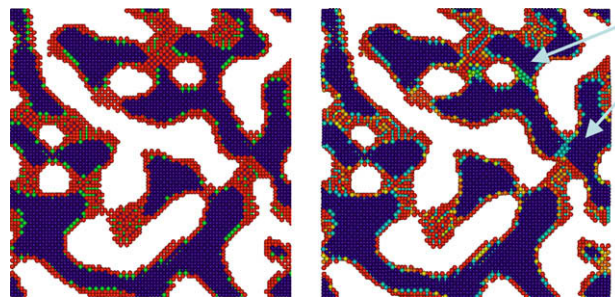


Figure 2. Slice through the structure relaxed with Au0 (left) and Au2 (right) color coded according to the centrosymmetry parameter where blue corresponds to the ideal face-centered cubic lattice, green corresponds to a stacking fault and red corresponds to the free surface. Plastic deformation induced by surface stress is indicated by the arrows. (For interpretation of the references to color in this figure legend, the reader is referred to the web version of this article.)

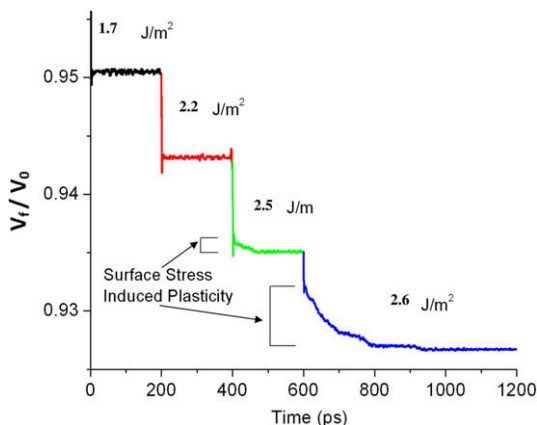


Figure 3. Relaxation curves for nanoporous gold. Volumetric strain for the 1.8 nm ligament sample after application of potentials Au0, Au1, Au2, and Au3, respectively. The value of the “isotropic” relaxed surface stress is indicated on the figure for reference (taken from Table 1).

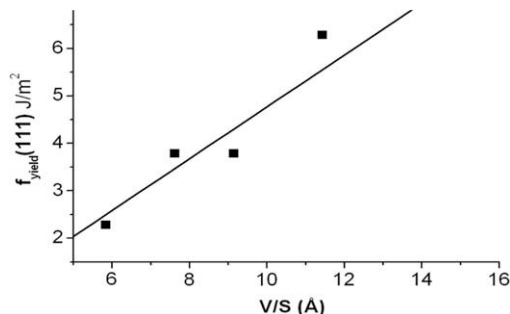


Figure 4. Critical unrelaxed {111} surface stress needed to initiate plastic deformation vs. the volume to surface area ratio with a corresponding slope given by $\frac{3}{2}(P)$. This yields a mean pressure of 3.7 GPa. The points correspond to the samples with ligament diameters of 1.5, 1.8, 2.1 and 2.7 nm. The samples with ligament diameters of 1.3 and 1.4 nm were unstable for all potentials used.

sure would not result in dislocation generation, indicating that capillary stress effects are not purely hydrostatic, in agreement with the analysis of Weissmuller and Cahn [16].

In summary, we have investigated the stability of nanoporous Au structures with very small ligament sizes. Experimentally, we report stable samples with ligament sizes down to 1.7 nm. We have created digital samples with ligament sizes from 1.3 to 3.6 nm. The structures of the samples created by our simulation technique compare very well with the experimental ones. Our digital samples are also very similar to those obtained by Rosner et al. [17] using electron tomography. In our atomistic simulations, we have used different interatomic potentials to mimic increasing values of the surface stress that may arise from charging the samples. The simulations show that spontaneous plasticity is observed, driven solely by the surface stress. Indeed, Schofield et al. [18] have shown that strain develops in nanoporous metallic films formed by dealloying. Crow-

son et al. [8] have investigated the role of the surface stress on the geometrical relaxation of nanoporous structures, and found significant effects. Our present results show that the effects of the surface stress can be sufficient to induce plasticity. Depending on the values of the surface stress, the surface stress induced plasticity can occur for different surface to volume ratios. Our simulations provide a critical value of the surface stress necessary to induce plasticity in a sample of a given surface to volume ratio. Our results also provide a possible explanation for the large volume change observed in experiments by Parida et al. [19].

S.G.C. acknowledges support by the National Science Foundation under Grant No. DMR-9975190 and DMR-0301007. D.F. acknowledges support by the NSF – Materials Theory. This work utilized Virginia Tech’s supercomputer and facilities supported in part by the National Science Foundation under Agreement No. DMR-9986442. The authors would also like to acknowledge the use of the code LAMMPS from Sandia National Laboratories and discussions with Karl Sieradzki, Joerg Weissmuller and Jonah Erlebacher.

- [1] S.G. Corcoran, in: S.D. Cramer, B.S. Covino Jr. (Eds.), ASM Handbook, Corrosion: Fundamentals, Testing, and Protection, vol. 13A, ASM International, Materials Park, OH, 2003, p. 287.
- [2] Y. Ding, Y.-J. Kim, J. Erlebacher, *Adv. Mater.* 16 (21) (2004) 1897.
- [3] J. Weissmuller, R.N. Viswanath, D. Kramer, P. Zimmer, R. Wurschum, H. Gleiter, *Science* 300 (5617) (2003) 312.
- [4] D. Kramer, R.N. Viswanath, J. Weissmuller, *Nano Lett.* 4 (5) (2004) 793.
- [5] K.F. Lin, T.R. Beck, *JECS* 123 (8) (1976) 1145.
- [6] J. Biener, A. Wittstock, L.A. Zepeda-Ruiz, M.M. Biener, V. Zielasek, D. Kramer, R.N. Viswanath, J. Weissmuller, M. Baumer, A.V. Hamza, *Nat. Mater.* 8 (1) (2009) 47.
- [7] X.Q. Feng, R. Xia, X. Li, B. Li, *Appl. Phys. Lett.* 94 (1) (2009) 3.
- [8] D.A. Crowson, D. Farkas, S.G. Corcoran, *Scripta Mater.* 56 (11) (2007) 919.
- [9] S.G. Corcoran, in preparation, 2009.
- [10] M. Haftel, M. Rosen, *Phys. Rev. B (Condensed Matter)* 64 (19) (2001) 195405/1.
- [11] M.I. Haftel, K. Gall, *Phys. Rev. B* 74 (3) (2006).
- [12] V. Fiorentini, M. Methfessel, M. Scheffler, *Phys. Rev. Lett.* 71 (7) (1993) 1051.
- [13] S. Plimpton, *J. Comput. Phys.* 117 (1) (1995) 1.
- [14] C.L. Kelchner, S.J. Plimpton, J.C. Hamilton, *Phys. Rev. B* 58 (17) (1998) 11085.
- [15] B. Hyde, H.D. Espinosa, D. Farkas, *JOM* 57 (9) (2005) 62.
- [16] J. Weissmuller, J.W. Cahn, *Acta Mater.* 45 (5) (1997) 1899.
- [17] H. Rosner, S. Parida, D. Kramer, C.A. Volkert, J. Weissmuller, *Adv. Eng. Mater.* 9 (7) (2007) 535.
- [18] E.J. Schofield, B. Ingham, A. Turnbull, M.F. Toney, M.P. Ryan, *Appl. Phys. Lett.* 92 (4) (2008) 3.
- [19] S. Parida, D. Kramer, C.A. Volkert, H. Rösner, J. Erlebacher, J. Weissmuller, *Phys. Rev. Lett.* 97 (2006) 035504.